

Room temperature quasi-brittle behaviour of an aluminous refractory concrete after firing

F. Simonin, C. Olagnon *, S. Maximilien, G. Fantozzi

GEMPPM, INSA-lyon, 69621 Villeurbanne Cedex, France

Received 16 November 2000; received in revised form 22 February 2001; accepted 7 March 2001

Abstract

The study deals with the thermomechanical behaviour of aluminous refractory concretes used in steel plants. In the temperature range where plasticity is negligible, the material presents a pronounced non linear behaviour both in uniaxial tensile and compressive modes, with a quasi brittle fracture. The behaviour is characterised by damage, firstly diffuse, then more localised, which finally leads to the formation of a macrocrack. The threshold of damage is very low in tension ($\approx 5\%$ of the maximum load) and higher in compression ($\approx 40\%$ of the maximum load). An approach, in terms of composite material, is proposed to analyse the damage behaviour. The concrete is, therefore, considered as a composite material, formed by coarse aggregates embedded in a fine matrix. The different mechanical behaviour observed between the matrix alone and the concrete can be explained by two phenomena : a structural temperature-independent effect and a temperature-dependent effect. Finally, the authors show that the real tensile behaviour of the refractory concrete, observed in the present work, is far from the description generally used in classical damage models. © 2001 Elsevier Science Ltd. All rights reserved.

Keywords: Calcium aluminates; Concrete; Fracture; Mechanical properties; Refractories

1. Introduction

The use of concrete as refractory material has been increasing recently.¹ One of the reasons for this is the relative ease of use, as compared to shaped materials. However, they have the intrinsic characteristic that they are heat treated in situ, which can present some disadvantages. Owing to the steady-state temperature gradient present in the installation, a gradient of temperature and thus of properties is present. In the moderate temperature range a drop of mechanical properties has been reported.^{2,3}

Concrete behaviour has often been considered as mostly linear and brittle. Structures in civil engineering are traditionally calculated on the sole base of the compressive strength values; the tensile strength being considered as nil.⁴

A detailed observation shows that such materials present a quasi-brittle behaviour, requiring a more accurate mechanical description including tensile and

compression behaviours. The last is easy to obtain but tensile properties are often deduced from bend tests. Although easy to conduct, the analysis is difficult for non-elastic behaviour. The real deformation can be measured by strain gages, but the stress can not be determined. Therefore, the tensile stress–strain curve can not be obtained without strong hypotheses or by comparison with models and inverse methods.⁵

The mechanical behaviour of concrete is related to the initiation and the development of cracks,^{6–8} which leads to some modelling difficulties. The models can be classified in continuum mechanics or discrete crack model.^{9,10} The former considers a diffuse damage that is treated as an effective modulus reduction. The first formulation was proposed by Kachanov.¹¹ The damage was initially quantified by a scalar parameter and more recently extended to anisotropic damage.¹² It can give a good description of the material if the damage is not localised. This is the case for concrete in the initial part of the stress–strain curve. The relevance of such models has also been shown by comparison with specific tests where localisation was prevented.^{13,14} Discrete models are derived from the fracture mechanics concept that have been modified to avoid the stress singularity. This

* Corresponding author.

E-mail address: christian.olagnon@insa-lyon.fr (C. Olagnon).

is the case of the fictitious crack model that includes a strain softening law linked to the fracture energy.¹⁵ Smeared crack models may be seen as a compromise between continuum mechanics and fracture mechanics. The main feature is the introduction of a plane of damage with a strain softening branch behaviour embedded in a continuum showing the undamaged behaviour.¹⁶

The damage has been shown to be caused by micro-cracking between the coarser aggregates and the rest of the material, the matrix, when considering concrete as a composite material. Specific micro-mechanical modelling has subsequently been proposed with this assumption. Although they can hardly be extended to structural prediction, they allow us to relate the behaviour to microstructural features.^{17–20} In the case of the refractory concrete, the firing has been shown to promote the initial damage of the material.^{21,22} In such a case, the non-linear behaviour can be accentuated and the material being considered as brittle is definitely erroneous. The determination of the real tensile characteristics appears, therefore, as necessary for the prediction of such material behaviour.

The purpose of this work is to analyse the quasi brittle mechanical behaviour of an alumina-spinel refractory material below 1000°C in order to see the adequacy with smeared crack models. For this purpose mechanical measurements were conducted at room temperature after different firing temperatures and the behaviour related to microstructural evolution.

2. Experiments

2.1. Material

The material studied in this work is a high-alumina concrete that contains 10 wt.% of synthetic spinel and 8 wt.% of aluminous cement. The raw-material content and the granulometry of each component are displayed in Table 1. As can be observed, the largest alumina aggregates are below 4 mm.

The concrete castable was prepared by mixing the raw materials with water (7 wt.% of the dry content). The mixed slurry was cast into molds and immediately placed in hermetic boxes, to avoid water evaporation. The material was cured for 24 h at a temperature of ≈

25°C. The cast specimens were heat-treated using a controlled cycle, to prevent initial cracking and spalling of the material caused by the excessive burn off of water. The initial heating rate was 20°C/h up to 110°C, followed by 30°C/h up to 450°C and 100°C/h to the firing temperature (from 110 up to 1600°C), which was maintained for 12 h. The cooling rate was about 300°C/h above 600°C and natural cooling below. The different specimens for mechanical testing were cast directly to the final shapes.

The concrete was considered as a composite material, constituted by large aggregates embedded in a matrix containing particles lower than 125 µm. So to analyse the role that the matrix has in regard to the thermo-mechanical behaviour of the concrete, samples of matrix were prepared from dry raw-material mixtures sieved to < 125 µm.

The evaluation of the phases and the microstructure of the materials with firing temperature were detailed in a former paper.²² However, an overview of the different mineralogic phases is given in Table 2. One can observe that above 600°C, there are no more hydrates. The crystallisation of mono-calcium aluminate ($\text{CaO} \cdot \text{Al}_2\text{O}_3$) and di-calcium aluminate ($\text{CaO} \cdot 2\text{Al}_2\text{O}_3$) starts at 900 and 1000°C, respectively and these compounds react to yield calcium hexaluminate $\text{CaO} \cdot 6\text{Al}_2\text{O}_3$ that crystallises above 1300°C.

2.2. Mechanical tests

The elastic modulus was measured on bars of dimensions 50×50×200 mm³, via the resonance method in flexure mode since very small displacements are induced by this method and no specimen damage occurs. Four-point bend tests were carried out on the same specimens with outer and inner spans of 182 and 67.5 mm respectively. They were tested at an imposed displacement rate of 0.1 mm/mn, and the load was recorded as a function of the maximum displacement, as measured using a linear variable displacement transducer (LVDT). To obtain a more accurate description of the mechanical behaviour, strain gauges were used in some cases. They were set on the tensile and compressive surfaces of bend bars along the beam axis, and they allowed the strain to be recorded directly with a good precision (±3%). For this purpose, a thin layer of epoxy resin was laid on the

Table 1
Raw materials contents and sizes

Supplier	Type	Content (wt.%)	Size	Matrix (< 125 µm)
Alcoa	Tabular alumina	41.34	1–4 mm	No
Péchiney	White corindon	30	0–2 mm	Partly
Alcoa	CA270 cement	8		Yes
Alcoa	Reactive alumina	10.5	< 20 µm	Yes
Alcoa	Mg-spinel AR78	10.13	< 20 µm	Yes

Table 2

Evolution of the mineralogical phases with firing temperature determined by X-ray diffraction^a

	T (°C)										
	110	450	600	900	1000	1100	1200	1300	1400	1500	1600
$\alpha\text{Al}_2\text{O}_3$	+++	+++	+++	+++	+++	+++	+++	+++	+++	+++	+++
$\beta\text{Al}_2\text{O}_3$	+	+	+	+	+	+	+	+	+	+	+
$\text{MgO} \cdot \text{Al}_2\text{O}_3$	+	+	+	+	+	+	+	+	+	+	+
$3\text{CaO} \cdot \text{Al}_2\text{O}_3 \cdot 6\text{H}_2\text{O}$	++										
$\text{Al}(\text{OH})_3$	++										
$12\text{CaO} \cdot 7\text{Al}_2\text{O}_3$		+	+								
$\text{CaO} \cdot \text{Al}_2\text{O}_3$				(1)++ ^b	+++	++	+				
$\text{CaO} \cdot 2\text{Al}_2\text{O}_3$					(2)+ ^c	++	+++	++	+		
$\text{CaO} \cdot 6\text{Al}_2\text{O}_3$								(3)+ ^d	++	+++	+++

^a (+) Low, (++) medium and (+++) high quantity.^b (1) Crystallization of mono calcium aluminate (CA).^c (2) $\text{CaO} \cdot \text{Al}_2\text{O}_3 + \text{Al}_2\text{O}_3 \rightarrow \text{CaO} \cdot 2\text{Al}_2\text{O}_3$ (CA₂).^d (3) $\text{CaO} \cdot 2\text{Al}_2\text{O}_3 + 4\text{Al}_2\text{O}_3 \rightarrow \text{CaO} \cdot 6\text{Al}_2\text{O}_3$ (CA₆).

surface and finely ground. The gauges were then fixed to the surface by an epoxy resin.

Compression tests were performed on cylinders with a diameter of 30 mm and a height of 50 mm. A grinding machine was used to make the two surfaces parallel. The tests were conducted at an imposed crosshead speed of 0.1 mm/min. The load was recorded as a function of the crosshead displacement which was corrected for the machine stiffness. The maximum compressive stress (σ_c) was calculated as the ratio of the maximum load to the cross-sectional area.

Some uniaxial tensile tests were also conducted. A cylindrical specimen of similar dimensions as that used for the compression test was glued with epoxy resin onto two steel cylinders. The sample and the steel grips were carefully centred, and the grips were fixed to the tensile machine through hole and pin. This allowed rotation about two axis to eliminate parasitic bending. On each specimen, 3 gauges were set parallel to the load axis at 120° to each other, in order to validate the test. An acoustic emission sensor was also connected to the specimen. The stress was calculated as the ratio of the maximum load to the cross-sectional area.

3. Results

Fig. 1 shows the typical curves obtained in the bend test with the strain gauges set onto both tensile and compressive faces. The behaviour appears strongly non-linear with a great asymmetry between tension and compression. Loading–unloading cycles show a typical damaging behaviour, with decreasing elastic modulus and increasing unrecoverable deformations.

To confirm this assumption, some incremental bend tests were conducted. Between each increment the specimen was unloaded and the elastic modulus was measured by the resonance method (Fig. 2). The variation of the elastic modulus gives a precise idea of the

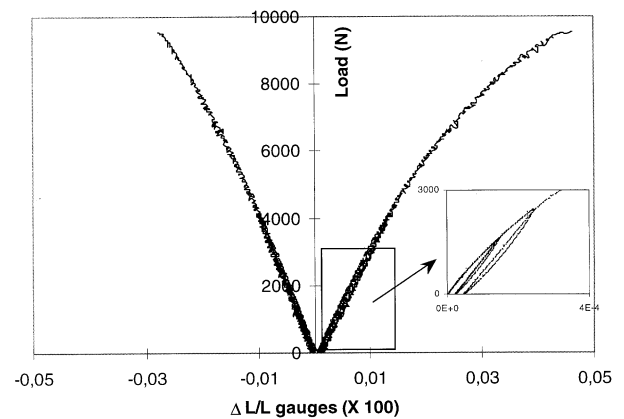


Fig. 1. Typical curves obtained in bending tests at room temperature after firing at intermediate temperature. Note the great dissymmetry between tensile and compressive faces.

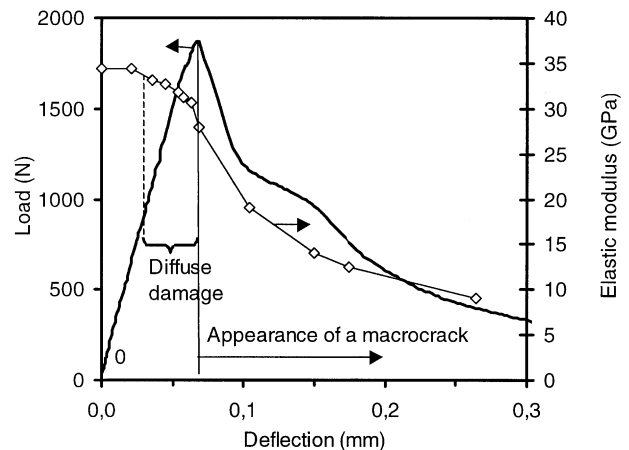


Fig. 2. Load–maximum displacement curve of the concrete fired at 450°C. The elastic modulus measured by resonance frequency characterises the damage evolution.

damage, that appears very early for a value half the maximum. It can be highlighted that the evolution of the slope of the load-displacement curve is far less sensitive

to detect the onset of damage. An attempt to observe the damage by in situ microscope observation clearly showed that a macroscopic crack appears at the maximum load. Furthermore, it corresponds to a significant decrease of the modulus. Therefore, this result suggests that, before the maximum load, a diffuse damage occurs, that probably coalesces, leading to the formation of a macro-crack and, therefore, localised damage.

The occurrence of the diffuse damage is strongly linked to the microstructure of the material, and therefore, to the heat-treatment temperature. Hence, the evolution of the elastic modulus and the maximum stress in bending presented in Fig. 3 shows a strong decrease between 110 and 450°C. This was attributed to the thermal expansion mismatches between the coarse aggregates and the fine matrix²² that induce an initial damage. Above 1000°C, owing to the crystallisation of the calcium aluminates and the consolidation, the heat treatment contributes to reduce the initial damage. This damage, leading to a asymmetry in tension-compression, can be quantified by comparison of the elastic modulus obtained in both tensile and compressive modes. The moduli were measured as ratio of the stress calculated from bend theory to the strain gage strains. There are relevant since measured at low stress (0.1 MPa i.e. in the linear part where no damage was observed in the tensile tests). The variation of the modulus difference with firing temperature is interesting (Table 3). Up to a firing temperature of 200°C, the difference is very small. After firing at 450°C, the difference in modulus strongly increases and can therefore be attributed to the damage of the specimen by diffuse microcracks due to the shrinkage mismatch. Indeed, damage plays a more significant role on the modulus in tensile mode than in compressive one. At higher firing temperatures, the difference is reduced by the sintering process which can lead to partial crack healing.

The compression behaviour for different heat treatments is represented in Fig. 4. In any case, one obtains a

Table 3

Relative difference of load-strain slopes measured on the tensile (E_t) and compressive (E_c) faces of a bend specimen

Firing temperature (°C)	Modulus difference ($E_c - E_t$) (%)
200	8 ± 3
450	30 ± 4
900	28 ± 4
1000	27 ± 4
1300	26 ± 4
1600	17 ± 5

non-linear behaviour associated to damage development. However, the more pronounced non-linear behaviour is obtained for the materials treated in the intermediate temperature range, between 450 and 1000°C, i.e. that exhibiting the highest initial damage.

Tensile tests have been conducted on concrete specimens after treatments of 110 and 450°C. As seen in Fig. 5, a pronounced non-linear behaviour was obtained. However, the variation of the non-linear behaviour with the heat-treatment temperature is even of greater amplitude than that obtained in compression. In any case the post-peak behaviour could not be obtained due to the non-stable nature of the test.

Performing a tensile test on a brittle material is always difficult, and a careful alignment of the specimen should be achieved to avoid bending. This was the case here, as shown in Fig. 6 where the three different curves corresponding to the strain gages are almost identical even up to large stress values. This also confirms the existence of diffuse damage within the specimen. When the load is very close to its maximum value, two of the three gauges suddenly record a higher strain. This indicates that the damage becomes more localised, leading to a macro-crack.

The onset of damage can be obtained by recording the acoustic emission during a tensile test. Fig. 7 shows the

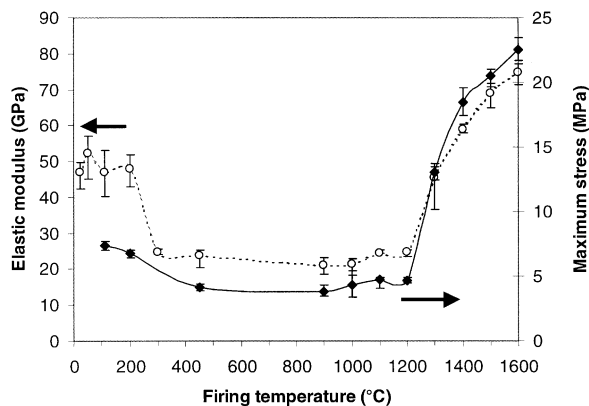


Fig. 3. Evolution of the elastic modulus and the maximum apparent stress measured in bending at room temperature, after firing at different temperatures.

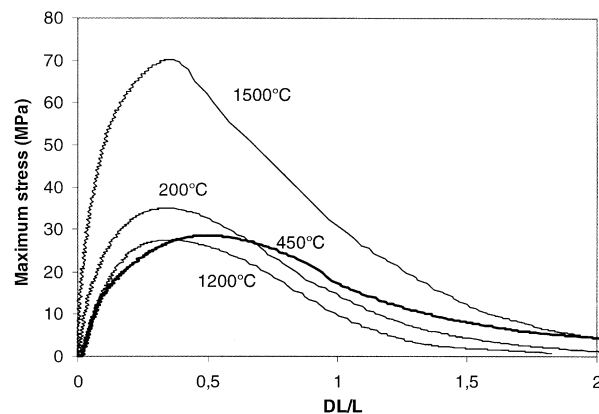


Fig. 4. Compression tests on concrete after firing at different temperatures.

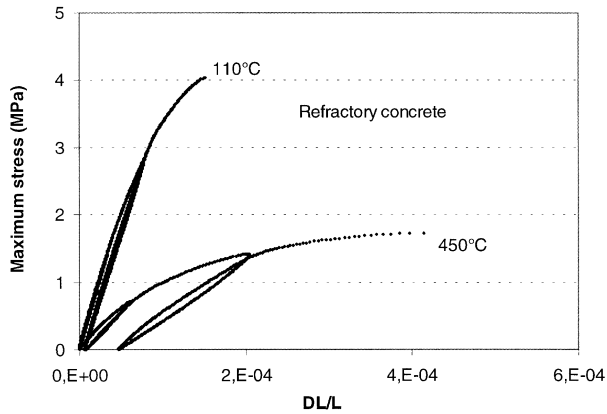


Fig. 5. Tensile tests on concrete at room temperature, after firing at different temperatures.

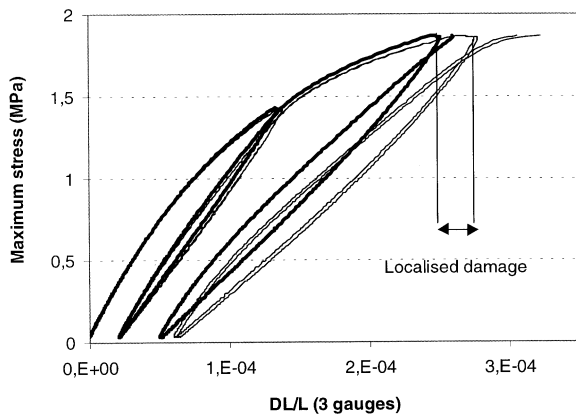


Fig. 6. Comparison of the behaviour recorded by the three different gauges on the uniaxial tensile test.

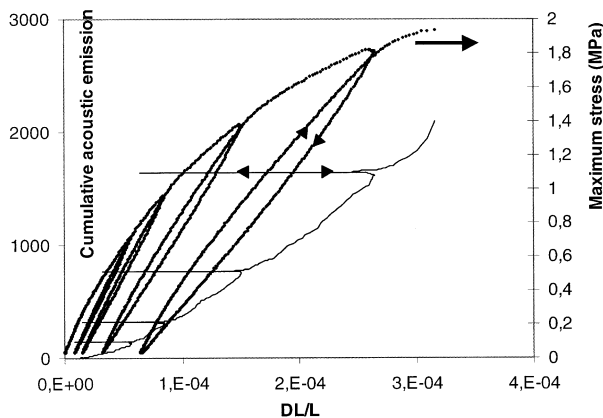


Fig. 7. Acoustic emission recorded during a tensile test, at room temperature.

cumulated number of events during loading. No event was detected during unloading or during further re-loading up to the former maximum value. Therefore, one can consider that the acoustic emission gives a good estimation of the damage. In this case of a specimen

treated at 450°C, the damage starts at very low stress, approximately 5% of the maximum value.

To analyse the role that the matrix has in regard to the thermomechanical behaviour of the concrete, tensile tests have also been conducted on matrix specimens after treatments of 110 and 450°C. The tensile behaviour for both concrete and cement samples fired at 110 and 450°C is schematically represented in Fig. 8. Whatever the firing temperature is, the damage is more in the concrete than in the matrix. Indeed, the mechanical behaviour of the matrix is close to an elastic linear behaviour.

In order to show that the tensile and compressive behaviours are relevant and representative of the real behaviour, one can model the flexure test from the tensile and compressive stress–strain behaviours. This can be easily done on a flexure test since no hypothesis of multi-axial behaviour is required. For this purpose a beam submitted to a constant moment was considered. The experimental tensile behaviour was fitted by a polynomial equation. In the range of the applied load of the bend test, the compressive behaviour can be supposed as elastic, with a very good approximation. The simulated results are presented in Fig. 9 in terms of load as function of compressive or tensile strain, and can therefore be directly compared to strain gauge result. There is a systematic discrepancy between the experimental measurement and the simulation. For a given load, the real deformation is about 30% higher. This can be explained by analysing the bending test in more details. Indeed, since the span to depth ratio is relatively low, the hypothesis of pure bending is not exact and the contribution of the shear force can not be neglected. This contribution could explain, at least to some extent the discrepancy therefore would need to be taken into account. However, the overall curve shapes are very similar, suggesting that the tensile stress–strain measurement is correct. In addition, it confirms that the description of the tensile behaviour directly from the load–tensile strain on the bend test is erroneous.

4. Discussion

The studied material presents a strong heterogeneity characterised by the presence of many defects (pores, microcracks...). The behaviour is therefore non linear both in uniaxial tensile and compressive modes. The threshold damage is very low in tension ($\approx 5\%$ of the maximum load) and higher in compression ($\approx 40\%$ of the maximum load).

The damage is present initially after the heat treatments but also develops under mechanical loading, inducing an increasing non linearity of the stress–strain curve. It is firstly characterised by a diffuse damage by microcracking, at the matrix–aggregates interface (which

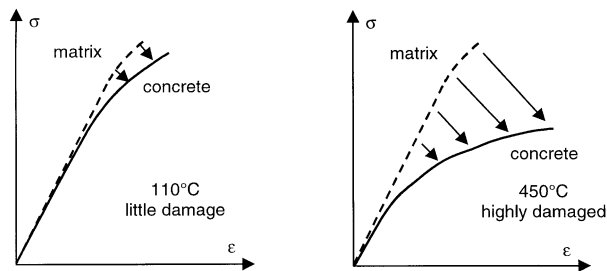


Fig. 8. Schematic representation of the behaviour of both concrete and matrix at different temperatures.

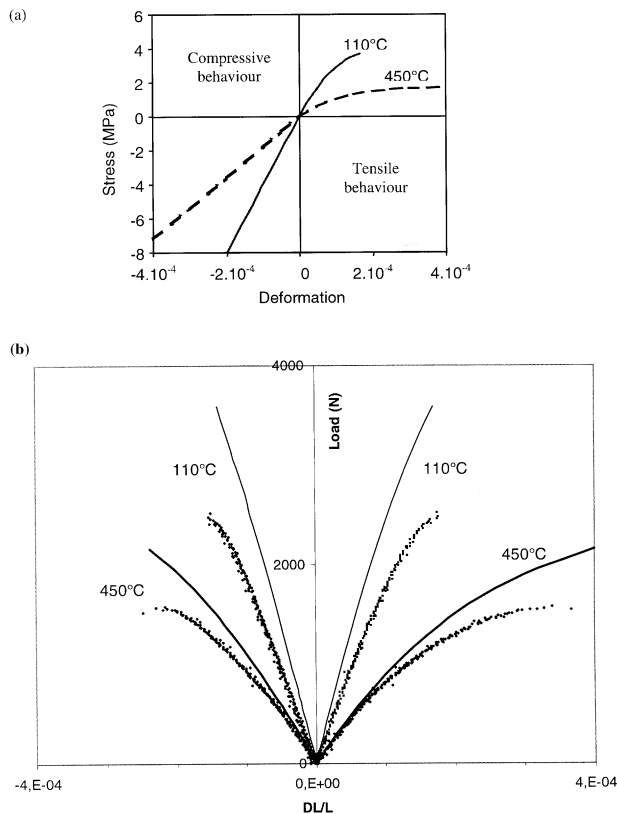


Fig. 9. (a) Uniaxial tensile and compressive curves; (b) comparison between the experimental bending curves (points) and the simulation (full line).

is the weakest zone), but also in the matrix. It is probable that the microcracks are initially homogeneously distributed, then more localised in some zones, either weaker or submitted to higher stresses. The creation of the microcracks, their opening and their propagation can be detected by recording the acoustic emission. During this first stage, the development of microcracks induces a reduction in the elastic modulus and an increase in the unrecoverable deformations. This damage by microcracking leads to a marked dissymmetry between tensile and compressive modes.

For higher loads, the damage becomes localised and is confined in a weak zone: the microcracks network then

connects and leads to the formation of a macrocrack that will control the fracture. Fig. 10 schematically describes the damage development on a load-displacement curve.

The comparison of the results for both the concrete and the matrix shows the importance of coarse aggregates on the damage behaviour. Indeed, the different results suggest that, compared to the matrix, the concrete presents a more pronounced non linear behaviour. This justifies the approach in terms of composite materials. The difference between the matrix and the concrete can therefore be explained by two phenomena : a structural effect, independent of the temperature, linked to elastic modulus difference and a temperature-dependent effect due the thermal expansion mismatches between matrix and aggregates.

One can suggest that damage appears earlier in the concrete during mechanical loading. This damage may be induced by local excessive stresses due to the difference in elastic modulus between aggregates (350 GPa) and matrix (30 GPa). The distributed nature of the size, the form and the arrangement of the aggregates leads to a great heterogeneity of the stress field : the damage is thus greatly distributed.

When the concrete is fired above 200°C, the damaging behaviour is more pronounced and develops from the pre-existing damage due to the thermal expansion mismatches. This damage can be represented as a distributed network of cracks (size and orientation). During loading, excessive stresses will appear in the vicinity of the cracks, because of their discontinuity and the local excessive stresses due to the “composite effect”. This leads to the same effect, a decrease of the elastic modulus, but more pronounced. For this reason, a highly non-linear behaviour is obtained.

In pure tension, the material presents a very low damage threshold value, corresponding to a very low stress value ($\approx 5\%$ of the maximum load). The behaviour is then highly non linear with an increase of the stress with increasing deformation. That means that in spite of the damage development, the stress continues to increase, which is, from a phenomenological point of view, similar to a pseudo work hardening. Therefore, phenomena of load-transfer do exist in the material, from damaged zones towards un-damaged ones.

It is, therefore, obvious to consider the real behaviour as greatly non-linear, even in pure tensile mode. To predict the behaviour of concrete structures, most of the continuum damage mechanics model state that the overall mechanical behaviour is driven by the tensile stress.

The materials, therefore, present higher characteristics in compression since high loads are require to initiate local tension. In classical damage models and particularly in the smeared crack model,²³ the tensile behaviour is generally described as linear elastic up to the initiation of the first damage, followed by a post peak decreasing

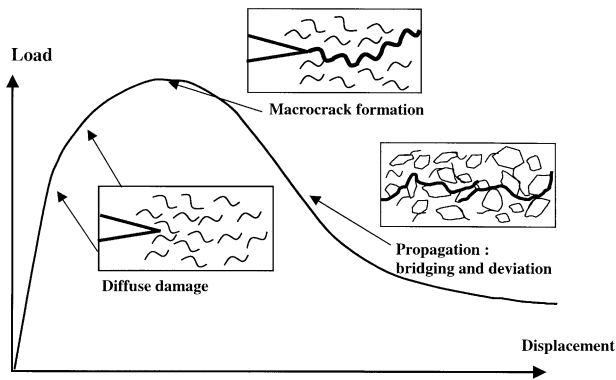


Fig. 10. Development of the damage on a notched beam in a bending test.

branch. Clearly the tensile behaviour observed in the present work (Fig. 5), and in agreement with some preceding works,^{24,25} is different from those classical models.

The authors have shown that it was possible to describe the global behaviour of a flexural test under smeared crack hypothesis.²² However, such a bending configuration is simple and the erroneous description of the tensile behaviour is compensated by the compressive zone. It is, therefore, doubtful that such a model could accurately describe any structural system made with a material presenting a so highly non-linear behaviour. For this purpose, one would need a mechanical model that would finely describe the real tensile behaviour, similar to that recently proposed by Shao et al.²⁶ for compression, and some efforts are required in this direction.

5. Conclusion

The refractory concrete presents a pronounced non-linear stress–strain behaviour, both in uniaxial tensile and compressive modes. It is initially caused by a diffuse damage constituted of a microcrack network. For higher loads or rather higher deformations, the damage becomes more localised in some zones and microcrack coalescence finally leads to the formation of a macrocrack that controls the final fracture.

The comparison of the thermomechanical results of both the concrete and the matrix shows the importance of coarse aggregates on the damage behaviour, justifying the analysis in terms of composite materials. The behaviour is the result of two phenomena: a global structural effect of the composite material, temperature-independent, linked to the elastic moduli difference and a firing temperature dependent effect due to thermal expansion mismatch. The initial damage is therefore strongly dependent on the firing temperature. This leads to very low threshold damage: 5 and 40% of the maximum load in tensile and compression loading respectively, as compared to concretes of Portland cement.

The tensile behaviour observed in this work can not be reasonably described by classical continuum mechanics damage models that consider the material as linear up to the initiation of the first damage.

Acknowledgements

Part of this work was carried out under a Brite Euram Project, Contract No. BRPR-CT 97-0427.

References

1. Lee, W. E. and Moore, R. E., Evolution of in situ refractories in the 20th century. *Journal of the American Ceramic Society*, 1998, **81**(6), 1385–1410.
2. Nonnet, E., Lequeux, N. and Boch, P., Elastic properties of high alumina cement castables from room temperature to 1600°C. *Journal of the European Ceramic Society*, 1999, **19**, 1575–1583.
3. Bazant, Z.P. and Kaplan, M.F., Concrete at high temperatures. Material properties and mathematical models. In *Concrete Design and Construction Series*. Longmann group, London, 1996, 404pp.
4. Baron, J., Le béton hydraulique. In *La Résistance à la Propagation de fissure*. Presses de l'Ecole Nationale des Ponts et Chaussées, Chapter. 18, Paris, 1982, pp. 317–333.
5. Mamdy-Andrieux, C., Analyse et simulation des contraintes d'origine thermique sur des structures réfractaires de centrales LFC, PhD Thesis from the University of Orléans, France, 1999, 172 pp.
6. Jensen, D. and Chatterji, S., State of the art report on micro-cracking and lifetime of concrete — Part I, Rilem technical committees, TC-122-MLC. *Matériaux et Constructions/Materials and Structures*, 1996, **29**, 3–8.
7. Harmuth, H., Rieder, K., Krobath, M. and Tschegg, E., Investigation of the non-linear behaviour of ordinary ceramic refractory materials. *Materials Science and Engineering*, 1996, **A214**, 53–61.
8. Henderson, R. J. and Chandler, H. W., The non-linear mechanical behaviour of high performance refractories. *Key Engineering Materials*, 1997, **132-136**, 504–507.
9. Heinfing, G., *Contribution à la modélisation du comportement du béton et des structures en béton armé sous sollicitation thermomécanique à hautes températures*. PhD thesis from the National Institute of Applied Sciences (INSA), Lyon, France, 1997, 209pp.
10. Krajcinovic, D. and Mastilovic, S., Brittle and quasi-ductile damage at large strain rates. *Theoretical and Applied Fracture Mechanics*, 2001, **35**, 9–18.
11. Kachanov, L. M., Time of the rupture process under creep conditions. *Izv. Akad. Nauk., SSR, Otd Tekh. Nauk*, 1958, **8**, 26–31.
12. Chaboche J. L., Continuum damage mechanics: I. General concepts, II. Damage growth, crack initiation and crack growth. *J. Appl. Mech.*, 1988, **55**, 59–72.
13. Berthaud, Y., Ringot, E. and Fokwa, D., A test for delaying localization in tension, Experimental investigation. *Cement and Concrete Research*, 1991, **21**, 928–940.
14. Bondon-Cussac, D., Hild, F. and Pijaudier-Cabot, G., Tensile damage in concrete: analysis of experimental technique. *J. Eng. Mech.*, August 1999, 906–913.
15. Hilleborg, A., Modéer, M. and Petersson, P. E., Analysis of crack formation and crack growth in concrete by means of fracture mechanics and finite elements. *Cement and Concrete Research*, 1976, **6**, 773–782.

16. Weihe, S., Kröplin, B., De Borst, R. and Classification of smeared crack models based on materials, structural properties, *Int. J. Solids Structures*, 1998, **35**(12), 1289–1308.
17. Huang, J. and Li, V. C., A meso-mechanical model of the tensile behaviour of concrete, part I: modelling the pre-peak stress-strain relation. *Composite*, 1989, **20**(4), 361–369.
18. Schlangen, E. and Van Mier, J. G. M., Simple lattice model for numerical simulation of concrete materials and structures. *Materials and Structures*, 1992, **25**, 534–542.
19. Huet, C., Guidoun, A. and Navi, P., *A 3D Micromechanical Model for Numerical Analysis and Prediction of Long Term Deterioration in Concrete under Severe Conditions: Environment and Loading*, Vol. II, ed. Sakai, Banthia and O.E. Gørr. 1995, E&FN Spon, pp.1458–1467.
20. Wang, J., Navi, P. and Huet, C. Numerical analysis of crack propagation in tension specimens of concrete as a 2D multi-cracked granular composite. *Materials and Structures*, **30**, 1997, 11–21.
21. Lemaistre, H., *Etude des propriétés thermomécaniques de divers réfractaires*. PhD thesis from the National Institute of Applied Sciences (INSA), Lyon, France, 1997, 127 pp.
22. Simonin, F., Olagnon, C., Maximilien, S., Fantozzi, G., Diaz, L.A. and Torrecillas, R., Thermo-mechanical behaviour of high alumina refractory castable with synthetic spinel additions. *Journal of the American Ceramic Society*, 2000, **83** (10), 2481–2490.
23. *Abaqus Theory Manual*. Hibbit, Karlsson, Sorrensen Version 5.7, 1996.
24. Evans, R. H. and Marathe, M. S., Microcracking and stress-strain curves for concrete in tension. *Materials and Structures Research and Testing (RILEM Paris)*, 1968, **1**(1), 61–64.
25. Marzouk, H. and Chen, Z. W., Fracture energy and tension properties of high-strength concrete. *Journal of Materials in Civil Engineering*, 1995, **7**(2), 108–116.
26. Shao, J. F. and Rudnicki, J. W., A microcrack-base continuous damage model for brittle geomaterials. *Mechanics of Materials*, 2000, **32**, 607–619.